JMEPEG (2010) 19:616–622
DOI: 10.1007/s11665-009-9519-2

1059-9495/$19.00

Effect of Solder Thickness on Electromigration Behavior in Eutectic SnPb Solder Reaction Couples

Guangchen Xu, Fu Guo, Zhidong Xia, Yongping Lei, Yaowu Shi, and Xiaoyan Li

(Submitted November 10, 2008; in revised form June 22, 2009)

The trend of miniaturization of electronic products induced the shrinking dimension of interconnects in the chip. When those interconnects are subjected to high current density (usually 10^3 to 10^4 A/cm^2), electromigration (EM) could affect the reliability of the chip which would ultimately break the circuit. In this study, eutectic SnPb solders with thickness of 280, 128, and 50 μm were investigated under high current density (10^4 A/cm^2) and high ambient temperature (120 °C). The EM-induced surface undulations were more prominent at the shorter thickness, demonstrating that the diffusion of metal atoms/ions was controlled by the actual temperature in the bulk solder instead of the back stress. Bamboo groove features were observed on the surface of solder extrusion at the anode side for the three solder thickness, which indicated the metal atoms/ions that migrated parallel to the direction of flow of electrons.

Keywords electromigration, eutectic SnPb, Joule heating, surface diffusion

1. Introduction

For high-performance electronic devices, the current trend is a wider application of flip chip technology to microprocessors and wireless handled electronic consumer products. Flip chip interconnects are used in the electric packaging manufacturing primarily because of their high input/output (I/O) density capacity, small profiles, and good electrical performance. It is expected that this interconnect technology will become even more important in the near future (Ref 1-3).

The popular composition for flip chip solder bumps before the year 2006 was eutectic SnPb solders. During recent years, it was replaced by Pb-free solders, such as Sn-Ag or Sn-Ag-Cu solders, due to the concerns about human health and environmental protection (Ref 4, 5). However, it was well recognized in certain electronic products, specifically servers, storage and storage array systems, network infrastructure equipment and network management for telecommunication equipment referred to as high-performance electronic products, the introduction of Pb-free materials would pose a significant potential reliability risk. Accordingly, the European Commission granted an exemption permitting the continued use of Pb in solders, independent of concentration, for high-performance equipment applications until year 2010 (Ref 6).

In flip chip packages, the number of I/O contact pads on a chip surface increased, the diameter of solder bumps decreased, and the current density through the contact area of a solder bump increased very rapidly. For example, flip chip interconnect with a 125 μm diameter and 250 μm pitch can form a full array of 2000 interconnects on a chip of 1×1 cm^2. If the diameter and pitch are reduced to 50 and 100 μm, respectively, 10,000 interconnects are possible on the chip. Current circuit design rules require that each interconnect carry a current of up to 0.2 A with an interconnect to 0.4 A in the near future. The current density will reach 10^4 A/cm^2 for the bump with 50 μm diameter (Ref 7-9). Thus, it is necessary to understand the EM behaviors in various solder thickness which could guide the future design rules of flip chip packages.

The currently popular joint configuration employed by the electronic manufacturers utilizes circuits with solder bumps. In such a configuration there exists an induced "current crowding" due to an extreme thin-thick divergence where local current densities can vary by two or more orders of magnitude over a very short distance (Ref 10, 11). In other words, in a real flip-chip joint, the movement direction of the atoms driven by thermal gradient will be along a direction opposite to that driven by electric current. In addition, the cross-interaction induced by the chemical potential between the two solder/pad interfaces could also drive the atoms of the base metal across the whole joint, where the movement of the atoms actually can also occur in a direction opposite to the electric current (Ref 12, 13). Therefore, it is difficult to carry out studies that isolate critical events due to the EM using the currently popular solder bump configuration. To minimize the current crowding, modifications to the joint geometry by adjusting the current path to be straight, and more uniform before entering the solder are being considered and adopted by industry. This paper deals with the development of an improved solder joint design—solder reaction couples (SRC)—that can be used to carry out some fundamentally critical studies on the effects of solder thickness on EM behavior both in lead-base and lead-free solder alloys.

2. Experimental Procedure

Although the straight V-groove samples having Cu wires as electrodes were introduced, the length of the solder line cannot

Guangchen Xu, Fu Guo, Zhidong Xia, Yongping Lei, Yaowu Shi, and **Xiaoyan Li**, College of Materials Science and Engineering, Beijing University of Technology, 100 Ping Le Yuan, Chaoyang District, Beijing 100124, P.R. China. Contact e-mails: xuguangchen@emails.bjut.edu.cn and guofu@bjut.edu.cn.

be well controlled by the spacing between the two Cu electrodes (Ref 14, 15). Therefore, an improved method was employed to solder the one-dimensional joints. The SRC with sandwich Cu/63Sn-37Pb/Cu structure was fabricated to conduct the study of EM behaviors. Two copper wires with 500 μm diameter were first put into a soldering die with U-grooves. And then, a 5 mg solder paste with 63Sn-37Pb composition was placed in the gap between two copper wires, as illustrated in Fig. 1(a). Finally, the die with the sample was heated up to 230 °C (50 °C higher than the melting point of 63Sn-37Pb) and then cooled down to room temperature rapidly by a fan. Figure 1(b) is the schematic drawing of the entire soldering set-up for the SRC. The solder thickness can be precisely controlled through spiral micrometer in the X-Y-Z translation stage. The as-reflowed SRC with three types of solder thickness were produced through this method whose sizes are 280, 128, and 50 μm. The as-reflowed SRC was then cold mounted in the epoxy resin, and, in order to raise the current density to a high level (10^4 A/cm^2), half dimension of the SRC was ground and polished off. Following this, a current of 10 A was continuously applied to the samples for 72 h; the corresponding current density in our experiment could reach to 10^4 A/cm^2. The samples were placed in an oven where temperature was set to 120 °C. Optical microscopy (OM) and scanning electron microscopy (SEM) were used to observe the microstructural and morphological evolution of the SRC, respectively. An energy-dispersive x-ray spectroscope (EDS) was used to analyze the compositions of the detected regions.

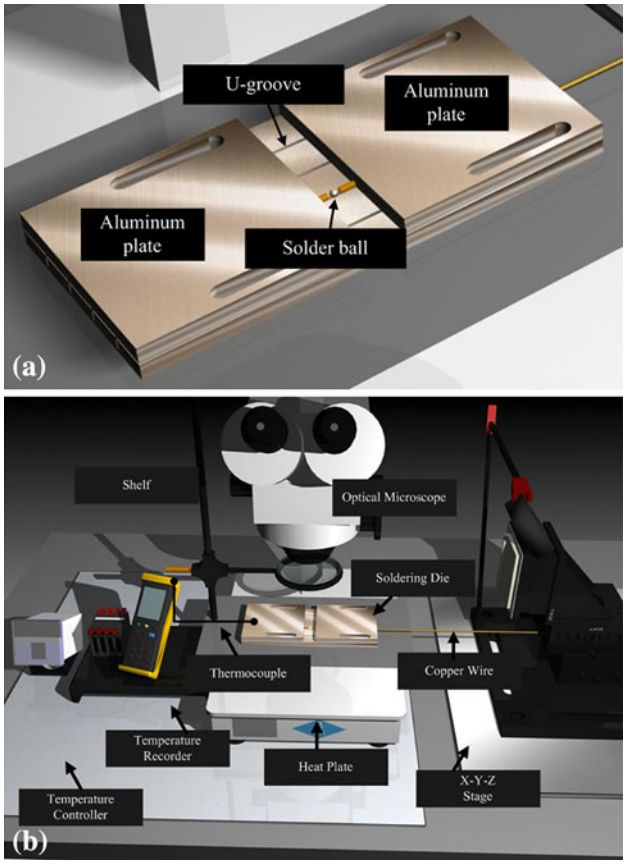

Fig. 1 (a) The solder die with U-grooves and (b) the entire soldering set-up for the SRC samples

3. Results and Discussion

3.1 Microstructure of the As-Reflowed SRC

It has been reported (Ref 16) that the as-reflowed solder has two different types of microstructure depending on their cooling rate. Alternating lamellae structure with Sn-rich phase and Pb-rich phase are observed when the cooling rate is slow. At faster cooling rates, the microstructure consists of two different phases of fine grains. As illustrated in Fig. 2, the temperature profile used to make the SRC samples was fixed during the re-flowing process. The microstructural features of the three types of as-reflowed SRC samples are similar to one another as illustrated in Fig. 3(a)-(c). There are two intermetallic compounds (IMC) of Cu and Sn; they are Cu_6Sn_5 and Cu_3Sn, and they form during the wetting reaction as well as the solid-state reactions between Sn and Cu according to the Cu-Sn binary phase diagram. The scallop-like Cu_6Sn_5 layer was the dominant IMC at the interface, while Cu_3Sn layer can seldom be found after the first re-flow process (Ref 16-19). Therefore, presence of a scallop-like Cu_6Sn_5 layer with an even thickness of about 2 μm can be noted in the Fig. 3(a)-(c). The as-reflowed SRC exhibits the classic inter-lamellar eutectic structure of Pb-rich and Sn-rich phases that are visible as white and grey domains, respectively, as illustrated in Fig. 3(d), which is the amplified image in Fig. 3(a). Pb-rich phase has significant (about 19%) solid solubility for Sn, while the Sn-rich phase has extremely low solid solubility for Pb (Ref 20). In addition, there are particles with sizes ranging from sub-microns to several microns scattered within the solder matrix, as illustrated in Fig. 3(c). These particles are identified to be Cu_6Sn_5 by EDS analysis.

3.2 Morphological Changes of the SRC After Current Stressing

After current stressing for 72 h, significant morphological changes had taken place in 280 μm-SRC, 128 μm-SRC, and 50 μm-SRC. As illustrated in Fig. 4(a), the greater region of the bulk solder in 280 μm-SRC was still flat. However, the surface at the anode side exhibits the bamboo groove structure which consists of rows of striations with spacing of several microns

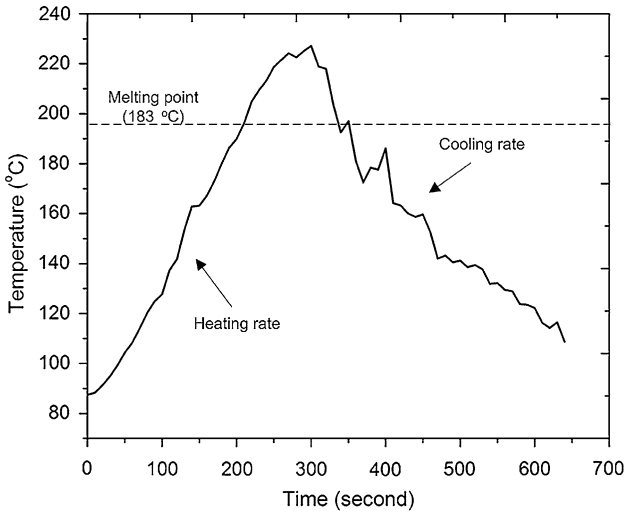

Fig. 2 Temperature profile of the soldering process

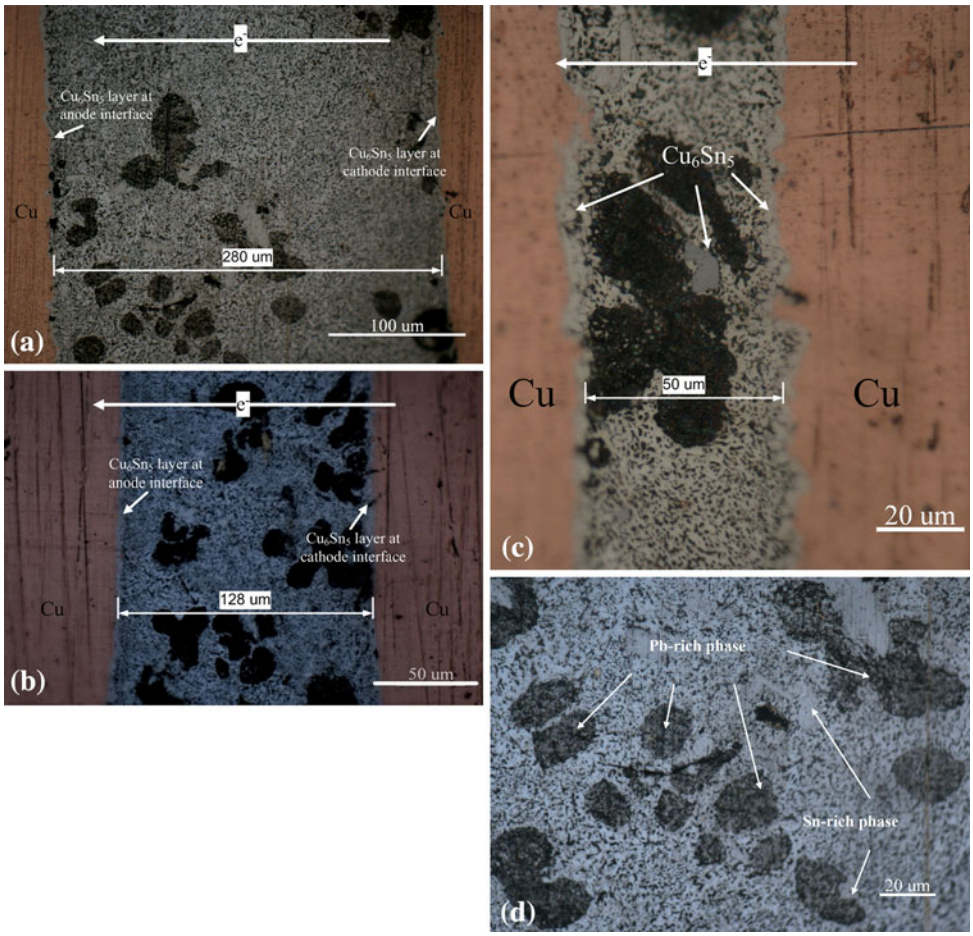

Fig. 3 The as-reflowed microstructure in the three types of solder thickness: (a) 280 μm-SRC, (b) 128 μm-SRC, (c) 50 μm-SRC, and (d) amplified image in (a)

after continuous current stressing as illustrated in Fig. 4(b), which is the amplified image of the inset in Fig. 4(a). In comparison to the situation for the 280 μm-SRC, the growth of the striations is different in 128 μm-SRC and 50 μm-SRC, as evidenced by SEM images provided in Fig. 5 and 6. Solder extrusion, which is like a curl sheet that capped on the copper substrate at the anode side, is observed in 128 μm-SRC as illustrated in Fig. 5(a). However, the solder extrusion in inset box 1 which is amplified to Fig. 5(b) does not cap on the copper substrate, which means it is in the initial stage. With applied current stressing resumed; the solder extrusion can continue to grow and eventually to cap on the surface of copper substrate. Like the flatness of 280 μm-SRC cross-section, the surface of 128 μm-SRC tends to be flat with no voids or valleys appearing. The solder matrix and copper substrate at cathode side exhibit good bond expect for the extrusion of Sn-Cu IMC at the interface, as illustrated in Fig. 5(c). In the 50 μm-SRC illustrated in Fig. 6(a), hillocks formed at the anode side while valleys formed at the cathode side simultaneously. There are also bamboo grooves on the surface of the hillock as illustrated in Fig. 6(b). It can be concluded that under high current density (10^4 A/cm^2) diffusion along the free surface can be the dominant diffusion path. In other words, the diffusion flux along the free surface is higher than that in the lattice. The formation of bamboo grooves can be considered as an indication of a material that is being squeezed out as a consequence of compressive stresses from EM-induced mass flow toward the anode.

3.3 Assessment of the Back Stress

The dependence of depletion on strip length was explained by the effect of back stress. In essence, when EM transports Al atoms in a strip from the cathode side to the anode side, the latter will be in compression and former in tension. On the basis of the Nabarro-Herring model of equilibrium vacancy concentration in a stressed solid, the tensile region has more and the compressive region has fewer vacancies than the unstressed region, so there is a vacancy concentration gradient decreasing from the cathode side to the anode side. The gradient induces an atomic flux of Al diffusing from the anode side to the cathode side, and it opposed the Al flux driven by EM from the cathode side to the anode side. The vacancy concentration gradient depends on the length of the strip; the shorter the strip, the greater the gradient. At a certain short length defined as the "critical length," the gradient is large enough to balance EM so no depletion at the cathode and no extrusion at the anode occur (Ref 16, 19).

Wei and Chen (Ref 21) found that no EM damage occurred for 5 and 10 μm stripes of eutectic SnPb under stressing by the current density of 2×10^4 A/cm^2 at 100 °C for 490 h, and the critical length was between 10 and 15 μm, which was close to

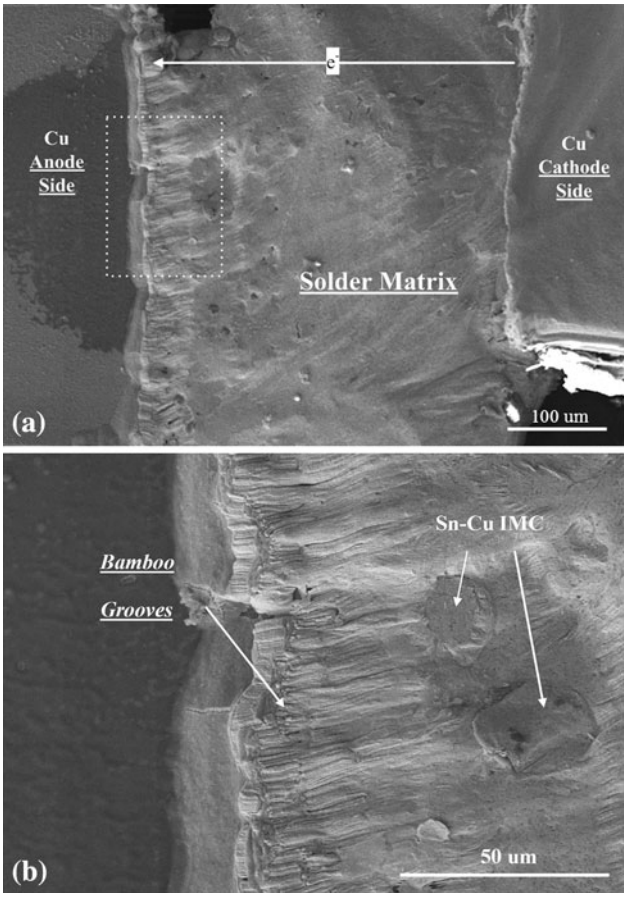

Fig. 4 (a) Morphological changes of the 280 μm-SRC after 72 h of current stressing and (b) bamboo grooves at the anode side

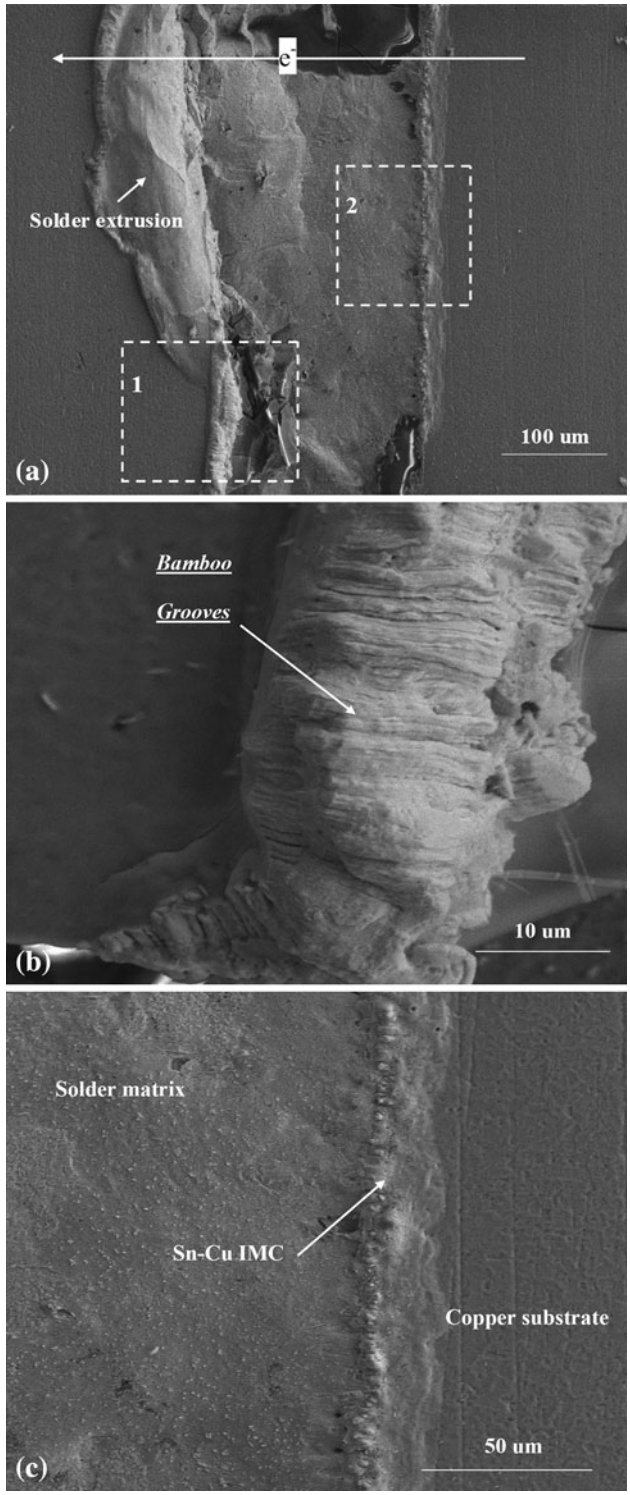

Fig. 5 (a) Morphological changes of the 128 μm-SRC after 72 h of current stressing, (b) bamboo grooves at the anode side in the dotted line box 1 in (a), and (c) morphological changes at the cathode side in the dotted line box 2 in (a)

their theoretical value of 11 μm. Ho et al. (Ref 22) noted significant amounts of surface undulations as a consequence of EM in 25 μm solder joints made of same material under similar conditions, indicating that EM was significant even when the joint thickness is very small.

In our present study, EM-induced surface undulations were more prominent in the SRC with shorter thickness. As stated in Sect 2, the samples, employed in the EM test, contained two different materials, which were copper substrates and the eutectic SnPb solder. Thus, there were two interfaces existing at the anode side and the cathode side where the incident electrons traveled in a direction normal to the interfaces, but the transmitted electrons bent in the normal direction to the interfaces. What's more, the interfaces exhibited the polarity effect at the anode side and the cathode side. When the incident electron impinged on the cathode interface, the transmitted electron could travel in a direction and make an angle to the normal, which could induce current crowding in the solder near the interface. Although the movement of every single electron was chaotic and random, this process occurred in an extremely short time due to the constant external field. In other words, the movement of electrons was aligned in the bulk solder. After a short period of movement, the electrons impinged on the anode interface, but at this time, the transmitted electrons crowded in the copper substrate. The current density threshold of copper is 10^6 A/cm^2, which was about two orders of magnitude more than required to cause EM failure in eutectic SnPb solders (Ref 1).

The current crowding at the dissimilar material interface could induce dramatic temperature increase. As illustrated in Fig. 7, the two heat sources (the interfaces) would conduct the extra thermal energy to the ambient air and the bulk solder, promoting the mobility of metal atoms/ions. EM is the result of

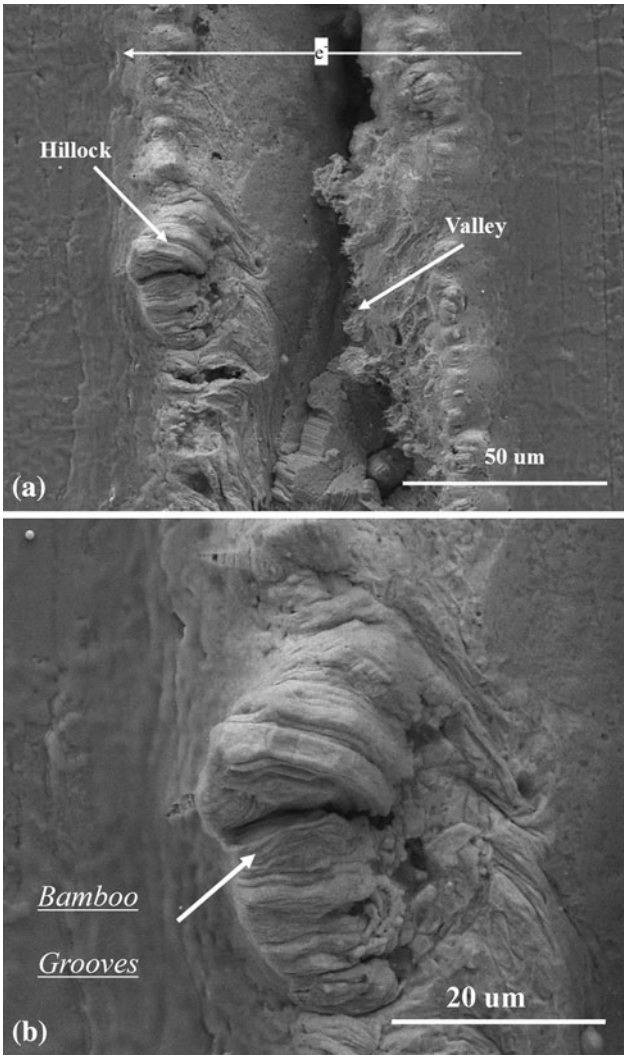

Fig. 6 (a) Morphological changes of the 50 μm-SRC after 72 h of current stressing and (b) bamboo grooves on the surface of hillock at the anode side

a combination of thermal and electrical effects on mass transport. Accordingly, temperature has a most profound influence on the diffusion coefficient and diffusion rates. The temperature dependence of diffusion coefficients is related to temperature according to

$$D = D_0 \exp\left(-\frac{Q_d}{RT}\right) \quad \text{(Eq 1)}$$

where D_0 is a temperature-independent preexponential (m^2/s), Q_d is the activation energy for diffusion (J/mol), R is the constant, and T is absolute temperature.

As shown in Fig. 8, the 280 μm-SRC have the largest heat dissipation area, enabling the temperature lower than the 128 μm-SRC and the 50 μm-SRC. Therefore, the EM-induced surface undulations were not distinct in the 280 μm-SRC, whereas the temperature in the 50 μm-SRC was much higher than the ambient temperature, enabling the formation of hillock and valley at the anode side and the cathode side, respectively.

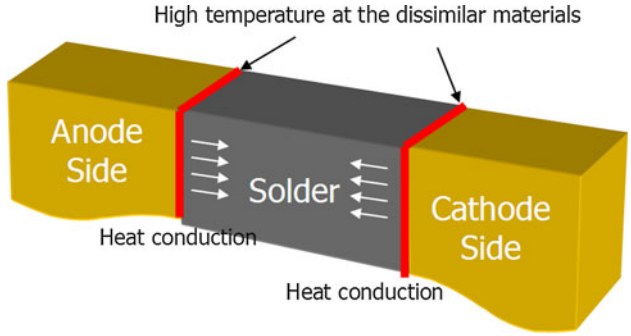

Fig. 7 Heat conduction from the dissimilar materials at the anode side and cathode side

In analyzing the atomic flux in the SRC, electron wind force and the mechanical force are considered to affect the motion of metal atoms/ions in solder at 120 °C (Ref 23):

$$J_{em} = -C\frac{D}{kT}\frac{d\sigma\Omega}{dx} + C\frac{D}{kT}Z^*eE \quad \text{(Eq 2)}$$

where J_{em} is the atomic flux in units of atom/cm^2 s, C the concentration of atoms per unit volume, D/kT the atomic mobility, σ the hydrostatic stress in the metal and $d\sigma/dx$ the stress gradient along the direction of electron flux, Ω the atomic volume, Z^* the effective charge number of EM, e the electron charge, and E the electric field.

By ignoring the back stress in our test and by measuring the atomic flux of EM, J_{em}, the equation can be expressed as:

$$J_{em} \approx C\frac{D}{kT}Z^*eE \quad \text{(Eq 3)}$$

The above equation can be written as

$$J_{em} \approx C\frac{D_0}{kT}\exp\left(-\frac{Q_d}{RT}\right)Z^*eE \quad \text{(Eq 4)}$$

Since C, D_0, k, R, Z^*, e, and E are all constants, J_{em} becomes the temperature-dependent atomic flux. Accordingly, when temperature increases, J_{em} increases at the same time.

4. Conclusions

We developed an improved design for the EM test which could effectively remove the influence of theromomigration and the hot spot induced by the current crowding. Eutectic SnPb SRC with three solder thicknesses that is subject to the high current density of 10^4 A/cm^2 at an ambient temperature of 120 °C was investigated. Solder extrusion with bamboo grooves at the anode side was observed at all three solder thicknesses. Free surface was the main diffusion path for atoms/ions that migrated from the cathode side to the anode side, and the migrating direction of metal atoms/ions in bulk solder was parallel to the movement of electrons. The bamboo grooves on the solder extrusion were squeezed out as a consequence of compressive stresses due to the block of copper substrates. In addition, the EM-induced surface undulations were more prominent at shorter thickness; this was caused by greater

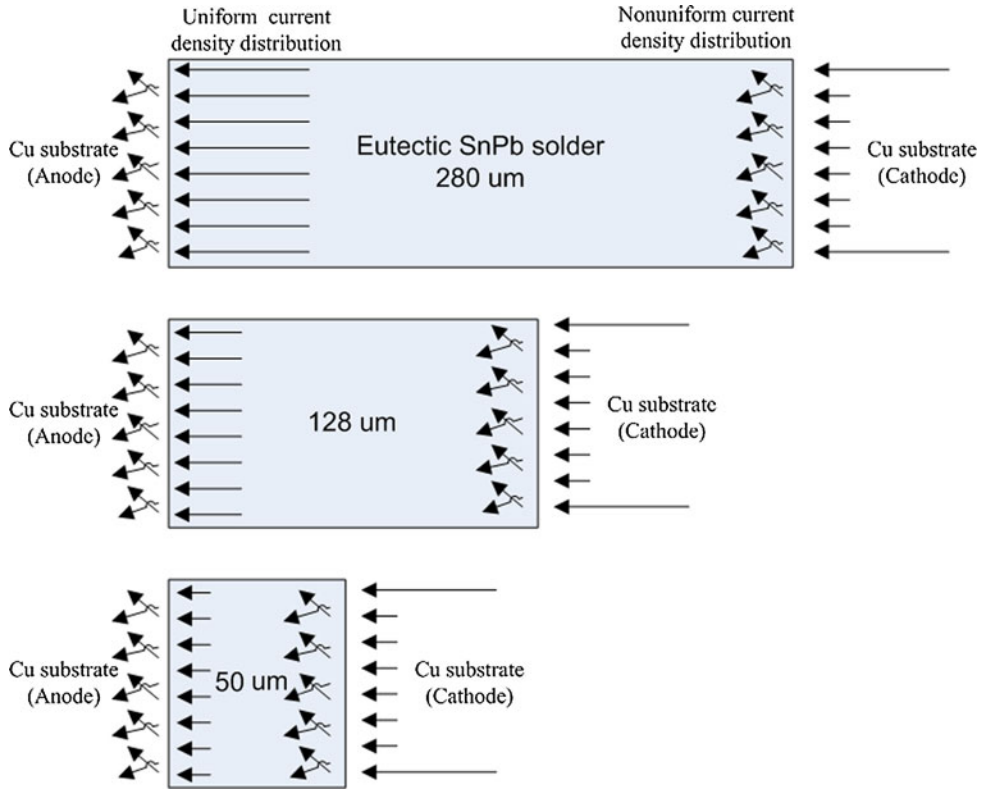

Fig. 8 The polarity effect of current density distribution among the three types of solder thickness

Joule heating effect due to the dissimilar materials at the two interfaces. However, the longer solder thickness had the larger heat dissipation area, enabling the temperature to drop as compared to the shorter solder thickness. Accordingly, the atomic flux could be enhanced by the higher actual temperature in the SRC. Thus, unlike the EM behaviors in the metal strip which excluded dissimilar materials at the anode side and the cathode side, the EM could cause more damage to the shorter solder thickness in the SRC. This had important implications to the reliability concerns of materials used in the flip chip technology.

Acknowledgments

The authors acknowledge the financial support of this work from the Beijing Natural Science Foundation Program and Scientific Research Key Program of Beijing Municipal Commission of Education (KZ200910005004), the Academic Innovation Group Supporting Program of Beijing Municipality.

References

1. K.N. Tu, Recent Advances on Electromigration in Very-Large-Scale-Integration of Interconnects, *J. Appl. Phys.*, 2003, **94**, p 5451–5473
2. Y.S. Lai, K.M. Chen, C.L. Kao, C.W. Lee, and Y.T. Chiu, Electromigration of Sn-37Pb and Sn-3Ag-1.5Cu/Sn-3Ag-0.5Cu Composite Flip-Chip Solder Bumps with Ti/Ni(V)/Cu Under Bump Metallurgy, *Microelectron. Reliab.*, 2007, **47**, p 1273–1279
3. M.O. Alam, B.Y. Wu, Y.C. Chan, and K.N. Tu, High Electric Current Density-Induced Interfacial Reactions in Micro Ball Grid Array Solder Joints, *Acta Mater.*, 2006, **54**, p 613–621
4. K. Yamanaka, Y. Tsukada, and K. Suganuma, Electromigration Effect on Solder Bump in Cu/Sn-3Ag-0.5Cu/Cu System, *Scr. Mater.*, 2006, **55**, p 867–870
5. B. Chao, S.H. Chae, X. Zhang, K.H. Lu, J. Im, and P.S. Ho, Investigation of Diffusion and Electromigration Parameters for Cu-Sn Intermetallic Compounds in Pb-Free Solders Using Simulated Annealing, *Acta Mater.*, 2007, **55**, p 2805–2814
6. K.J. Puttlitz and G.T. Galyon, Impact of the ROHS Directive on High-Performance Electronic Systems—Part II: Key Reliability Issues Preventing the Implementation of Lead-Free Solders, *J. Mater. Sci.: Mater. Electron.*, 2007, **18**, p 347–365
7. Y.L. Lin, Y.S. Lai, C.M. Tsai, and C.R. Kao, Effect of Surface Finish on the Failure Mechanisms of Flip-Chip Solder Joints Under Electromigration, *J. Electron. Mater.*, 2006, **35**, p 2147–2153
8. C.M. Tsai, Y.S. Lai, Y.L. Lin, C.W. Chang, and C.R. Kao, In-Situ Observation of Material Migration in Flip-Chip Solder Joints Under Current Stressing, *J. Electron. Mater.*, 2006, **35**(10), p 1781–1786
9. S.W. Liang, Y.W. Chang, and C. Chen, Relieving Hot-Spot Temperature During Electromigration in Solder and Current Crowding Effects Bumps by Using Cu Columns, *J. Electron. Mater.*, 2007, **36**, p 1348–1354
10. L. Zhang, S. Ou, J. Huang, K.N. Tu, S. Gee, and L. Nguyen, Effect of Current Crowding on Void Propagation at the Interface Between Intermetallic Compound and Solder in Flip Chip Solder Joints, *Appl. Phys. Lett.*, 2006, **88**, p 012106(1)-(3)
11. E.C.C. Yeh, W.J. Choi, K.N. Tu, P. Elenius, and H. Balkan, Mean-Time-to-Failure Study of Flip Chip Solder Joints on Cu/Ni(V)/Al Thin-Film Under-Bump-Metallization, *Appl. Phys. Lett.*, 2002, **80**, p 5665–5671
12. T.Y. Lee, K.N. Tu, S.M. Kuo, and D.R. Frear, Electromigration of Eutectic SnPb Solder Interconnects for Flip Chip Technology, *J. Appl. Phys.*, 2001, **89**, p 3189–3194
13. J.W. Nah, K.W. Paik, J.O. Suh, and K.N. Tu, Mechanism of Electromigration-Induced Failure in the 97Pb-3Sn and 37Pb-63Sn Composite Solder Joints, *J. Appl. Phys.*, 2003, **94**, p 7560–7566
14. S. Ou and K.N. Tu, *Proceedings of the 55th Electronic Components and Technology Conference* (Piscataway, NJ), IEEE, 2005, p 1445–1450
15. M. Lu, P. Lauro, D.-Y. Shih, R. Polastre, C. Goldsmith, D.W. Henderson, H. Zhang, and M.G. Cho, *Proceedings of the 58th*

Electronic Components and Technology Conference (Piscataway, NJ), IEEE, 2008, p 360–365
16. K.N. Tu and K. Zeng, Tin-Lead (SnPb) Solder Reaction in Flip Chip Technology, *Mater. Sci. Eng. R*, 2001, **34**, p 1–58
17. B. Li, Y. Shi, Y. Lei, F. Guo, Z. Xia, and B. Zong, Effect of Rare Earth Element Addition on the Microstructure of Sn-Ag-Cu Solder Joint, *J. Electron. Mater.*, 2005, **34**, p 217–224
18. I.A. Blech, Electromigration in Thin Aluminum Film on Titanium Nitride, *J. Appl. Phys.*, 1976, **47**, p 1203–1208
19. K.N. Tu, Electromigration in Stressed Thin Films, *Phys. Rev. B*, 1992, **45**, p 1409–1413
20. A. Lee, C.E. Ho, and K.N. Subramanian, Electromigration Induced Microstructure and Morphological Changes in Eutectic SnPb Solder Joints, *J. Mater. Res.*, 2007, **22**, p 569–574
21. C.C. Wei and C. Chen, Critical Length of Electromigration for Eutectic SnPb Solder Stripe, *Appl. Phys. Lett.*, 2006, **88**, p 182105(1)-(3)
22. C.E. Ho, A. Lee, and K.N. Subramanian, Design of Solder Joints for Fundamental Studies on the Effects of Electromigration, *J. Mater. Sci.: Mater. Electron.*, 2007, **55**, p 569–574
23. K.N. Tu, *Solder Joint Technology: Materials, Properties, and Reliability*, Springer, New York, 2007